Effect of Zinc Borate on the Fire and Thermal Degradation Behaviors of a Poly(3-hydroxybutyrate-*co*-4-hydroxybutyrate)-Containing Intumescent Flame Retardant

Rui Zhang,[1] Hua Huang,[1] Wei Yang,[2] Xifu Xiao,[1] Yuan Hu[2]

[1]*College of Chemical Engineering, Nanjing Forestry University, Nanjing, Jiangsu 210037, People's Republic of China*
[2]*State Key Laboratory of Fire Science, University of Science and Technology of China, Hefei, Anhui 230026, People's Republic of China*

Received 19 August 2011; accepted 27 November 2011
DOI 10.1002/app.36533
Published online in Wiley Online Library (wileyonlinelibrary.com).

ABSTRACT: The aim of this study was to investigate the effect of zinc borate (ZnB) on the fire and thermal degradation behaviors of a poly(3-hydroxybutyrate-*co*-4-hydroxybutyrate) [P(3,4)HB]-containing intumescent flame retardant (IFR). The IFR system was composed of ammonium polyphosphate, pentaerythritol, and melamine. The fire properties of P(3,4)HB/IFR/ZnB blends were evaluated by limited oxygen index, Underwriters Laboratories 94, microscale combustion calorimetry (MCC), and cone calorimetry (CONE) testing. The results of MCC and CONE show that the peak heat release rate, which is an important indicator of material fire hazard, of P(3,4)HB/IFR decreased when a small amount of the IFR was substituted by ZnB. The thermal degradation behavior of the P(3,4)HB/IFR/ZnB blends were measured by thermogravimetric analysis and thermogravimetric analysis–infrared (TG–IR) spectrometry. The data of TG–IR showed that the flammable gas products of P(3,4)HB released during the thermal degradation process were greatly decreased. Scanning electron microscopy analysis revealed that more compact char residues were observed with the incorporation of ZnB. © 2012 Wiley Periodicals, Inc. J Appl Polym Sci 000: 000–000, 2012

Key words: blends; flame retardance; intumescence; polyesters; thermal properties

INTRODUCTION

Because of emerging environmental concerns and petroleum resource exhaustion resulting from nondegradable petroleum-based plastics, there has been considerable interest in biodegradable polymeric materials.[1] Poly(3-hydroxybutyrate-*co*-4-hydroxybutyrate) [P(3,4)HB] is one biodegradable polymer; it belongs to the polyhydroxyalkanoate family, which can be synthesized by at least 75 different genera of bacteria, such as *Alcaligenes eutrophus* and *Pseudomonas oleovorans*, as an intracellular reserve energy compound like cane sugar.[2–4] Because of its biocompatibility, biodegradability, and outstanding mechanical properties, P(3,4)HB is expected to replace some common petroleum-based plastics in industrial, medical, and agricultural fields.[5,6] Although P(3,4)HB has been found to be suitable for industrial applications, its high combustibility and serious dripping during combustion limit its further application in some particular areas. Thus, it is necessary to develop flame-retardant P(3,4)HB systems.

There are two usual ways to improve the flame retardancy of polymeric materials, including additive and reactive approaches. Additive-type flame retardants are the most commonly used through incorporation into polymers by physical form, which is convenient for material fabrication.[7] Additive-type flame retardants mainly contain halogen-containing flame retardants, phosphorus-containing compounds, nitrogen-containing flame retardants, and inorganic additives.[8] Halogen-containing flame retardants show remarkable efficiency, but they have obvious disadvantages; for example, they may generate toxic and corrosive fumes during incineration, which can lead to environmental problems.[9] Therefore, it is necessary to develop halogen-free flame retardants to avoid these disadvantages. Among halogen-free flame retardants, intumescent flame retardants (IFRs) are well known for their high efficiency and have been used in various polymers, including petroleum-based polymers, because of their advantages of little smoke and low toxicity.[10,11] IFRs are composed of three components: an acid source, a carbon source,

Correspondence to: R. Zhang (zhrlm@ustc.edu).
Contract grant sponsor: High-Level Talent Project of Nanjing Forestry University; contract grant number: G2009-01.
Contract grant sponsor: Project Funded by the Priority Academic Program Development of Jiangsu Higher Education Institutions (2010).

and a blowing agent.[12] The formulation of IFRs, which have been widely used, consists of ammonium polyphosphate (APP), pentaerythritol (PER), and melamine (MA).[13] When IFR materials are heated, they can swell and form a foamed cellular charred layer on the surface, which plays the role of heat insulator, oxygen barrier, and smoke suppressor.[14,15] A mechanism can be postulated: that the charred layers acting as a physical barrier can slow down heat and mass transfer between the gas and condensed phases.[16]

However, IFRs have some shortcomings, such as low thermal stability, water solubility, and high addition dosage.[17] To overcome some of these defects, a number of synergistic agents have been proposed. Zinc borate (ZnB), one of those synergistic agents, is usually used in flame-retardant polymers to improve their flame retardancy, such as suppressing smoke, extinguishing dripping, promoting charring and so on.[16,18] There have some reports on the flame-retardant behavior of ZnB in polyethylene/IFR and polypropylene/IFR systems, which have shown that the addition of a small amount of ZnB can remarkably improve the flame retardancy.[18–22] It is well known that ZnB can form a ceramic-like protective layer and promote the formation of char during burning; this results in better fire performance.[23]

Although IFR and ZnB have excellent fire retardancy that can be widely used in petroleum-based polymers, there is little information available in the literature on the flame-retardant behavior of polyhydroxyalkanoates. This work was mainly devoted to the investigation of the effect of IFR and ZnB on the flame retardancy of P(3,4)HB. The IFR system and ZnB were blended with P(3,4)HB to obtain flame-retardant and ecofriendly materials. The flame-retardant properties of the P(3,4)HB blends containing flame retardant were evaluated by limited oxygen index (LOI), Underwriters Laboratories (UL) 94, microscale combustion calorimetry (MCC), and cone calorimetry (CONE) testing. The thermal degradation behavior of the P(3,4)HB/IFR/ZnB blends were measured by thermogravimetric analysis (TGA) and thermogravimetric analysis–infrared (TG–IR) spectrometry. The morphologies of the char residue were analyzed by scanning electron microscopy (SEM).

EXPERIMENTAL

Materials

The biodegradable P(3,4)HB copolymer was provided from Tianjin Green Bioscience Co., Ltd. (Tianjin, China) in the form of a powder containing about 5% 4-hydroxybutyrate (4HB), with a melt flow index of 3 g/10 min (based on ASTM 1238-906; 2.1 kg loaded at 170°C). APP-II, PER, and ZnB in the form of powders were kindly supplied by Wuhu Keyan Chemical Materials Co., Ltd. (Wuhu, China). MA was obtained from the China Medicine (Group) Shanghai Chemical Reagent Corp. (Shanghai, China). IFR was a blend of APP, PER, and MA with a mass ratio of 3 : 1 : 1.

Flame-retardant P(3,4)HB blend preparation

In this work, the mass ratio of APP, PER, and MA was fixed at 3 : 1 : 1. P(3,4)HB and all of the additives were dried at 80°C for at least 24 h before use. All of the samples were prepared on a two-roll mill (XK-160, Changzhou No.1 Rubber&Plastic Equipment Co., Ltd, Changzhou, China) at 150°C for 10 min, and the roll speed was kept at 50 rpm. The resulting samples were then molded with a hot press at 170°C into sheets 3.0 mm thick. Seven different formulations were prepared, as shown in Table I.

Characterization and measurements

TGA was performed under flowing nitrogen (60 mL/min) on a DTG-60AH thermogravimetric analyzer (Shimadzu, Kyoto, Japan) at a heating rate of 20°C/min. About 5–10 mg samples, placed in a Pt pan, were heated from ambient temperature to

TABLE I
Formula and TGA and DTG Data for the Neat P(3,4)HB and Its Composites

Sample	P(3,4)HB (wt %)	IFR (wt %)[a]	ZnB (wt %)	$T_{-5\%}$ (°C)	$T_{-50\%}$ (°C)	T_{max} (°C)	Residue (wt %) 400°C	500°C	600°C
P(3,4)HB-0	100	0	0	277	292	289	1.0	0	0
P(3,4)HB-1	85	15	0	273	307	306	11.1	8.6	6.1
P(3,4)HB-2	80	20	0	269	306	304	14.2	11.3	8.4
P(3,4)HB-3	75	25	0	268	304	301	17.0	12.5	9.1
P(3,4)HB-4	70	30	0	266	303	298	20.7	15.5	9.8
P(3,4)HB-5	75	24.5	0.5	265	303	298	15.7	12.3	9.6
P(3,4)HB-6	75	24	1	268	302	298	17.7	14.2	12.3
P(3,4)HB-7	75	23	2	264	297	292	17.5	14.8	13.3

[a] The composition of IFR was APP/PER/MA = 3 : 1 : 1 (mass ratio).

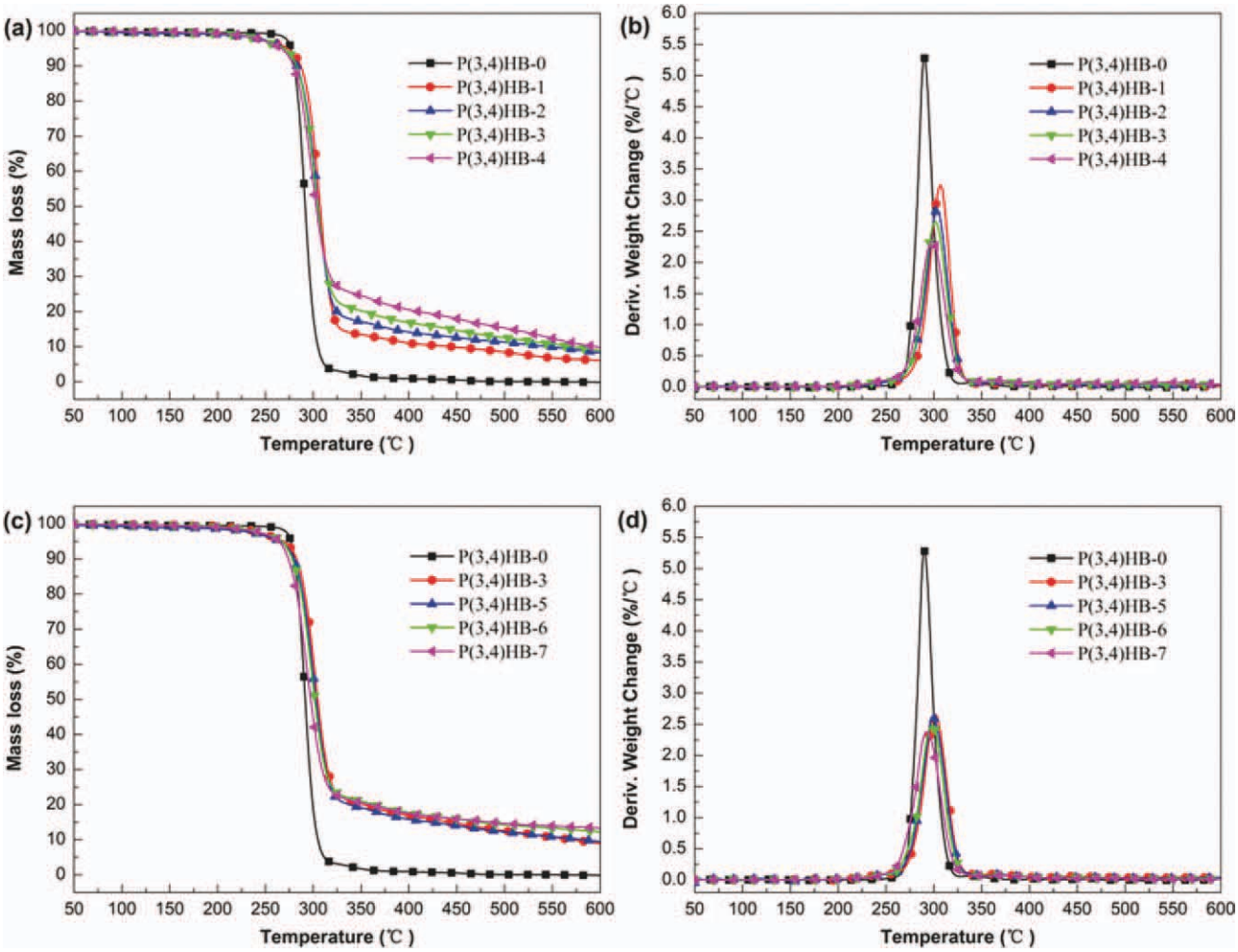

Figure 1 TGA and DTG curves of (a,b) neat P(3,4)HB and P(3,4)HB/IFR and (c,d) the P(3,4)HB/IFR/ZnB composites. [Color figure can be viewed in the online issue, which is available at wileyonlinelibrary.com.]

700°C. The specimens were tested in duplicate under the same conditions, and the average values are reported; the temperature was reproducible to ±1°C, and the mass was reproducible to ±0.2%.

TG–IR spectrometry was carried out with a TGA Q5000 IR thermogravimetric analyzer (TA Instruments Waters, Shanghai, China) linked to a Nicolet 6700 FTIR spectrophotometer (Nicolet Instruments, Madison, USA). The weights of all of the samples were kept at 5.0 mg. Samples in an alumina crucible were tested in a nitrogen atmosphere (flow rate = 60 mL/min) at temperatures ranging from 30 to 700°C at a heating rate of 20°C/min.

LOI and UL 94 testing were used to study the flammability properties of the samples. LOI values were measured with an HC-2 oxygen index meter (Jiangning Analysis Instrument Co., China) according to the ASTM D 2863 oxygen index method with test specimen bars (100 × 6.5 × 3 mm). UL 94 vertical testing was carried out with a CFZ-2-type instrument (Jiangning Analysis Instrument Co., Nanjing, China) with test specimen bars (130 × 13 × 3 mm).

The thermal combustion properties were tested on a microscale combustion calorimeter (MCC-2, GOVMARK) according to ASTM D 7309-07. In the test, samples of about 5 mg were heated to 650°C at a linear heating rate of 1°C/s in a stream of nitrogen (80 mL/min). The gaseous thermal degradation products were mixed with a stream of oxygen (20 mL/min) before entering a 900°C combustion furnace. The heat release rate (HRR) was calculated by the amount of oxygen depletion measured with an oxygen analyzer.

CONE testing was carried out with a Stanton Redcroft CONE instrument (East Grinstead, UK) according to ISO-5660 standard procedures. All of the samples were put in a horizontal orientation under a heat flux of 35 kW/m^2, and the specimen size was 100 × 100 × 3 mm. Typical results from CONE were reproducible within ±10%.

The morphologies of the char residue of the P(3,4)HB blends after LOI testing were observed with a Hitachi X650 scanning electron microscope (Tokyo, Japan) at an accelerating voltage of 20 kV.

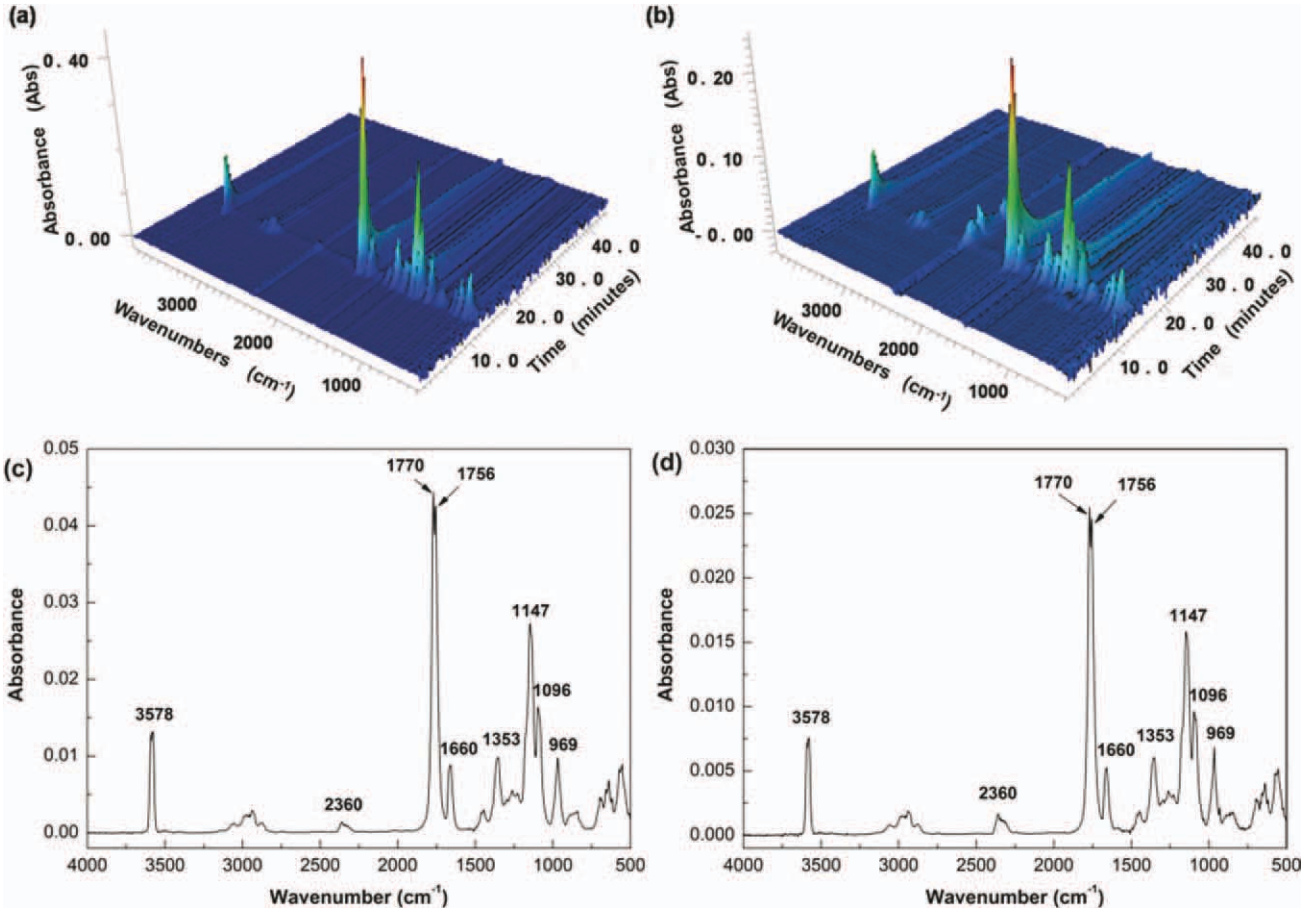

Figure 2 Three-dimensional surface graph for the FTIR spectra of the evolved gases produced and FTIR spectrum of pyrolysis products at the maximum decomposition rate for (a,c) P(3,4)HB-0 and (b,d) P(3,4)HB-5. [Color figure can be viewed in the online issue, which is available at wileyonlinelibrary.com.]

The surfaces of the tested specimens were sputter-coated with a thin layer of gold before the measurement.

RESULTS AND DISCUSSION

TGA

The TGA and differential thermogravimetry (DTG) curves of the neat P(3,4)HB and its blends are shown in Figure 1. The 5 and 50% weight loss temperatures ($T_{-5\%}$ and $T_{-50\%}$, respectively), maximum decomposition temperature (T_{max}), and char residues at 400, 500, and 600°C are all summarized in Table I. As shown in Figure 1(a,b) and Table I, P(3,4)HB-0 underwent one-step degradation in the range of total weight loss, in which the onset weight loss temperature ($T_{-5\%}$) and T_{max} were around 277 and 289°C, respectively, and there was no char residue at 500°C. When the IFR was added to P(3,4)HB, $T_{-5\%}$ decreased about 4–11°C. The reduction of the starting thermal stability was probably related to the decomposition of APP around 215°C, which could have released gases such as NH_3 and H_2O, and the decomposition of PER and MA around 277 and 250°C, respectively.[10,24] Moreover, in the presence of IFR, the $T_{-50\%}$ and T_{max} of the P(3,4)HB/IFR blends were obviously higher than those of P(3,4)HB-0. It could also be seen that the P(3,4)HB/IFR blends were more thermally stable than neat P(3,4)HB when the temperature exceeded 280°C, and the maximum mass loss rate was remarkably reduced during the stage of decomposition. Furthermore, the char residue increased with the addition of IFR; for example, at 400°C, the undecomposed parts of P(3,4)HB-1 to P(3,4)HB-4 were 11.1, 14.2, 17.0, and

TABLE II
Characteristic Attributions of the FTIR Absorption Bands

Band position (cm^{-1})	Assignment
2360	CO_2
1770, 1660, 1147, 1096	Unsaturated ester
3578, 1756, 1660, 969	Unsaturated carboxyl acid
1660	Propene

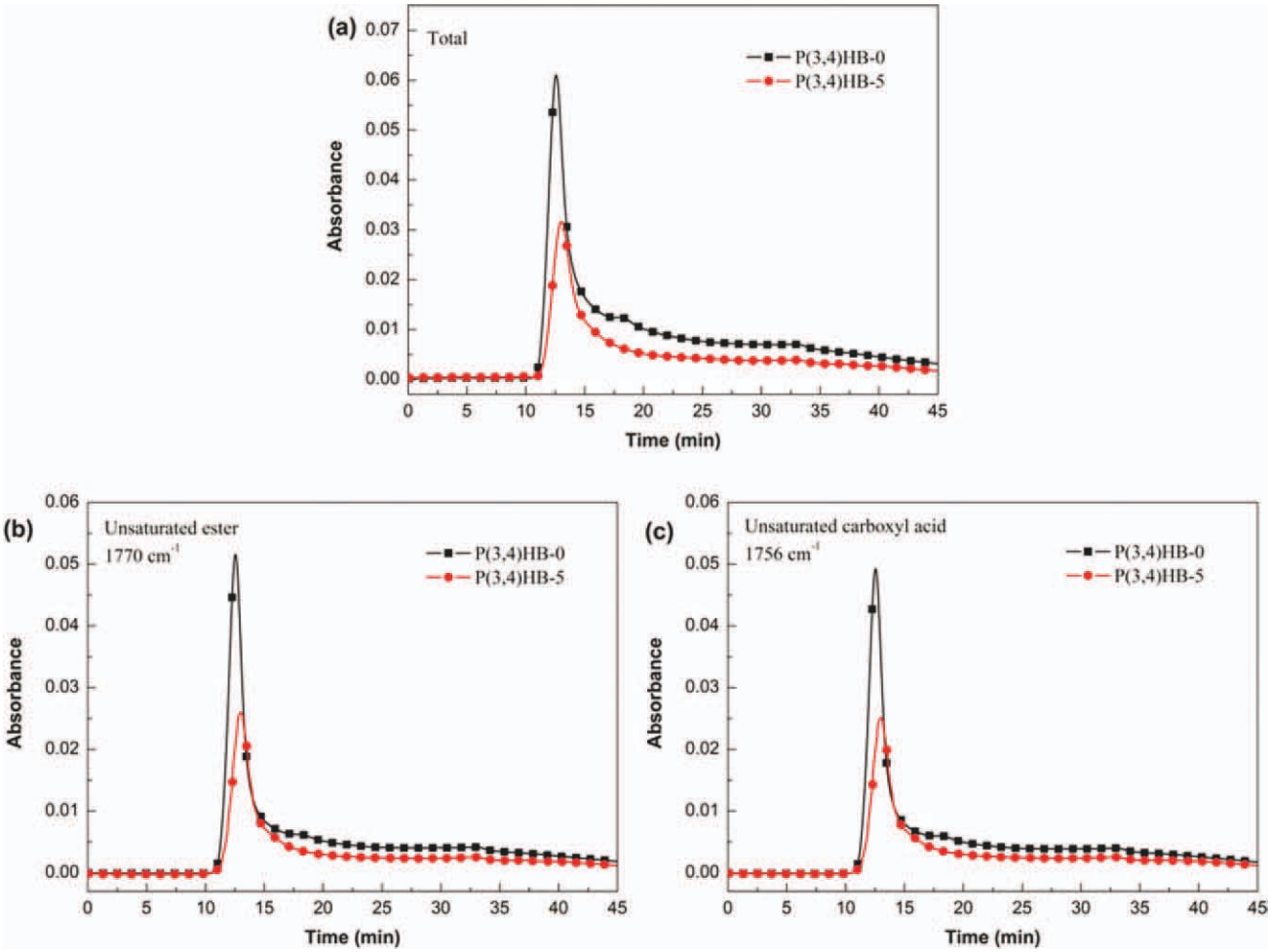

Figure 3 Absorbance of the pyrolysis products for P(3,4)HB-0 and P(3,4)HB-5 versus time: (a) total, (b) unsaturated ester, and (c) unsaturated carboxyl acid. [Color figure can be viewed in the online issue, which is available at wileyonlinelibrary.com.]

20.7%, respectively, whereas P(3,4)HB-0 decomposed almost completely. The amount of the char residue of the P(3,4)HB/IFR system was still higher than 6.1%, even at 600°C. As shown in Figure 1(c,d), the additive quantity was controlled at 25 wt % with a small amount substitution of ZnB; the TGA curves of P(3,4)HB-3 and P(3,4)HB/IFR/ZnB almost overlapped when the temperature was below 450°C. However, the maximum mass loss rate of the P(3,4)HB/IFR/ZnB system dropped, and the amount of char residue at 600°C increased in comparison with P(3,4)HB-3. This was because ZnB formed a ceramic-like protective layer to protect the char, which played a role in heat protection and the elimination of oxygen to decrease the oxidization speed at high temperatures.[18]

Decomposition production analysis

TG–FTIR spectroscopy is an effective testing method for understanding the thermal decomposition mechanism by analysis of the gas products. The three-dimensional TG–IR spectra of gas phase in the thermal decomposition of P(3,4)HB-0 and P(3,4)HB-5 are shown in Figure 2(a,b). To understand the change in the volatilized products, the FTIR spectra of the pyrolysis products P(3,4)HB-0 and P(3,4)HB-5 at

TABLE III
Results of UL 94 and LOI Testing for the Neat P(3,4)HB and Its Composites

Sample	LOI	UL 94, 3.0 mm bar		
		t_1/t_2	Dripping	Rating
P(3,4)HB-0	20.5 ± 0.5	BC	Yes/yes	NR
P(3,4)HB-1	24 ± 0.5	BC	Yes/yes	NR
P(3,4)HB-2	26 ± 0.5	7.1/2.5	No/yes	V-2
P(3,4)HB-3	27 ± 0.5	5.7/8.0	No/no	V-1
P(3,4)HB-4	28.5 ± 0.5	1.1/1.7	No/no	V-0
P(3,4)HB-5	28 ± 0.5	1.0/7.7	No/no	V-0
P(3,4)HB-6	27 ± 0.5	1.0/8.6	No/no	V-0
P(3,4)HB-7	25 ± 0.5	1.0/4.6	No/no	V-0

t_1 and t_2, average combustion times after the first and the second applications of the flame, respectively; BC, burns to clamp; NR, not rated.

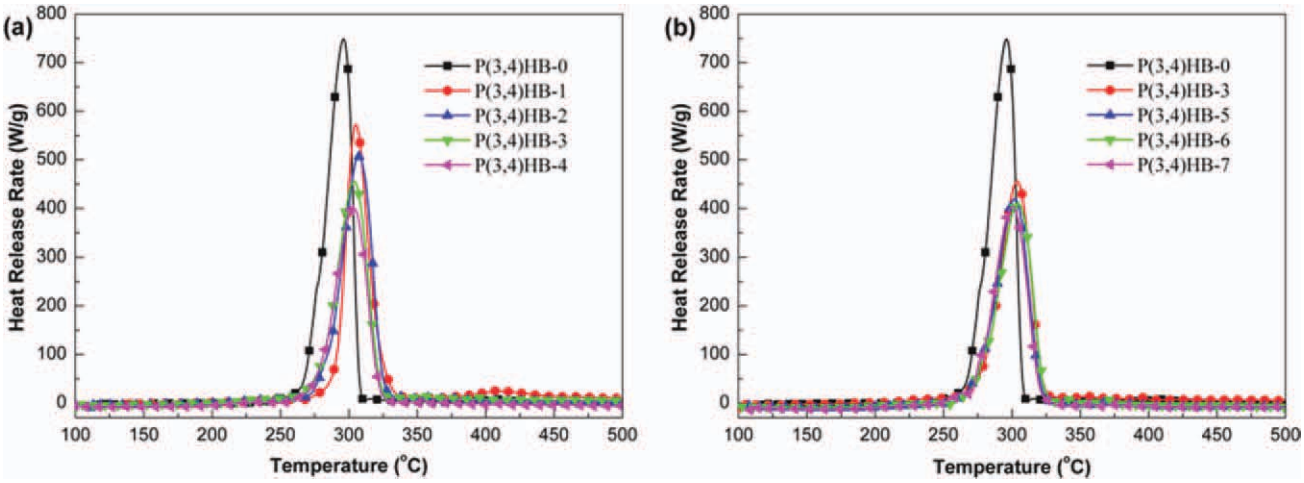

Figure 4 HRR curves of the (a) P(3,4)HB/IFR and (b) P(3,4)HB/IFR/ZnB systems obtained from MCC. [Color figure can be viewed in the online issue, which is available at wileyonlinelibrary.com.]

maximum decomposition rates are shown in Figure 2(c,d). The main signals from the gas phase spectra are assigned and summarized in Table II.

As shown in Figure 2, the adsorption bands of P(3,4)HB-0 and P(3,4)HB-5 were similar, and the main evolved gases of the thermal degradation of P(3,4)HB-0 and P(3,4)HB-5 were compounds including —OH (carboxyl group, 3578 and 969 cm^{-1}), CO_2 (2360 cm^{-1}), —C=O (unsaturated ester and unsaturated carboxyl acid, 1770 and 1756 cm^{-1}), —C=C— (1660 cm^{-1}), $—CH_3$ (1353 cm^{-1}), and —C—O— (esters, 1147 and 1096 cm^{-1}). The main decomposition products were CO_2, unsaturated ester, unsaturated carboxyl acid, and propene.[25]

To further investigate the intensity changes of some representative groups, the absorbance of pyrolysis products versus time for P(3,4)HB-0 and P(3,4)HB-5 are presented in Figure 3. The absorbance intensity of the total gas, unsaturated ester, and unsaturated carboxyl acid for P(3,4)HB-0 and P(3,4)HB-5 are shown in Figure 3(a–c), respectively. It can be seen that all of the peaks of the absorbance intensity for P(3,4)HB-5 were lower than those for P(3,4)HB-0. In fact, the combustible products of P(3,4)HB-5 were reduced by nearly half in comparison with those of neat P(3,4)HB. Consequently, the IFR combined with ZnB observably reduced the combustible gas and the weight loss and led to the improvement of the flame retardancy of the P(3,4)HB matrix.

LOI and UL 94 testing

The flame-retardant properties of the neat P(3,4)HB and its blends were studied by LOI and UL 94 testing. The tests results are presented in Table III. It can been seen that the neat P(3,4)HB and P(3,4)HB-1 were easy to burn, with serious dripping in the application of the flame, so there was no rating in the UL 94 testing. The sample for P(3,4)HB-2 was extinguished after the removal of flame in two applications, but it had dripping during the second flame application; thus, P(3,4)HB-2 achieved a V-2 rating. For P(3,4)HB-3 and P(3,4)HB-4, the UL 94 testing reached V-1 and V-0 ratings, respectively. According to Table I, the LOI values of the P(3,4)HB/IFR blends [P(3,4)HB-0∼ P(3,4)HB-4] increased from 20.5 ± 0.5 to 28.5 ± 0.5 with increasing IFR. These results indicate that IFR (APP/PER/MA = 3 : 1 : 1) obviously improved the flame retardancy of P(3,4)HB.

The relationship between the content of ZnB and the flame retardancy of the P(3,4)HB/IFR blends is also shown in Table III. The total amount of additives remained at 25 wt %, and the substitution of part of IFR by ZnB further improved the flame retardancy of P(3,4)HB/IFR. Compared with P(3,4)HB-3, the LOI values at first increased to a maximum value (28 ± 0.5) when 0.5 wt % ZnB was added, but the LOI value decreased with further increases in the content of ZnB. When the content of

TABLE IV
MCC Results for the Neat P(3,4)HB and Its Composites

Sample	PHRR (W/g)	THR (kJ/g)	HRC (J g^{-1} K^{-1})	T_{PHRR} (°C)
P(3,4)HB-0	748.6	17.7	714	296.2
P(3,4)HB-1	572.1	14.9	553	305.2
P(3,4)HB-2	508.7	15.6	501	307.4
P(3,4)HB-3	455.5	14.6	454	303.4
P(3,4)HB-4	408.4	13.0	409	303.1
P(3,4)HB-5	419.1	14.1	430	302.1
P(3,4)HB-6	418.1	13.7	421	304.4
P(3,4)HB-7	412.2	12.6	412	300.4

HRC ± 5 J g^{-1} K^{-1}; PHRR ± 5 W/g; THR ± 0.1 kJ/g; T_{PHRR} ± 2°C.

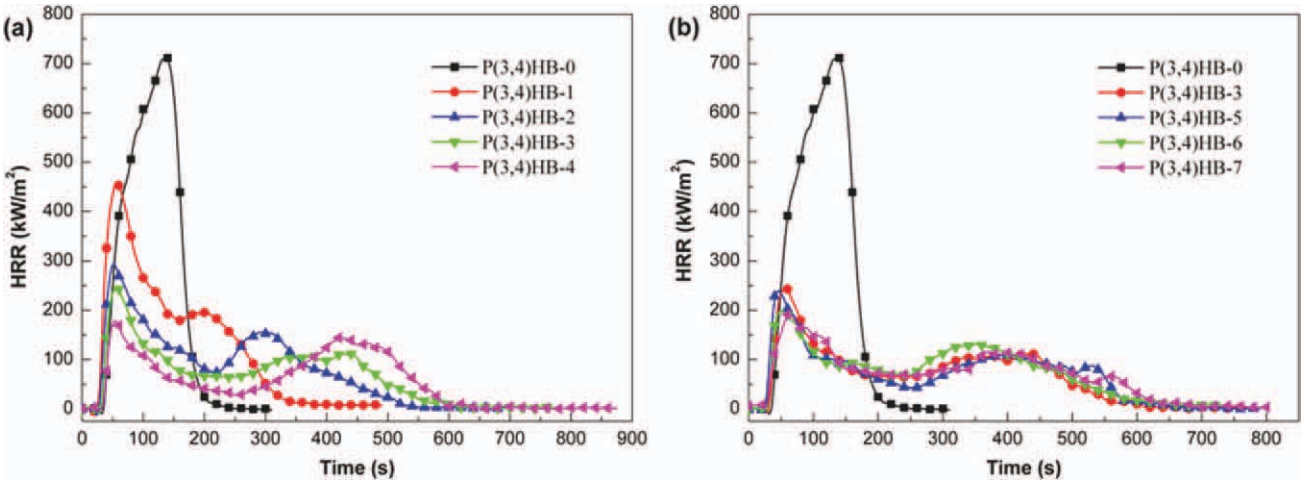

Figure 5 HRR curves of the (a) P(3,4)HB/IFR and (b) P(3,4)HB/IFR/ZnB systems obtained from CONE. [Color figure can be viewed in the online issue, which is available at wileyonlinelibrary.com.]

ZnB was between 0.5 and 2 wt %, a UL 94 testing V-0 rating was reached, the samples hardly ignited in the first flame application, and the flame time in UL 94 testing was remarkably reduced. These data indicated that there existed a synergistic effect between ZnB and the IFR system at a low content of ZnB, and this significantly enhanced the flame retardancy of P(3,4)HB.

MCC testing

MCC is a new, rapid, small-scale flammability testing method that can be used to study polymer combustion properties on milligram quantities, whereas CONE requires large quantities (25–100 g) of polymer materials for precise and repeatable determinations.[26] Both MCC and CONE measurement methods were used to cross-validate the results, with the aim of providing robust data.

For MCC, the HRR curves of P(3,4)HB and its blends are given in Figure 4, and the corresponding combustion data are summarized in Table IV. As shown in Figure 4(a), the peak heat release rate (PHRR) values of the P(3,4)HB/IFR system was significantly reduced with the addition of the IFR content. Compared with P(3,4)HB-0, the PHRR value of P(3,4)HB-4 with 30 wt % IFR was reduced by around 45%. The heat release capacity (HRC) and total heat release (THR), which are important parameters for evaluating the flame hazards of a material, were also reduced, and the temperature at the peak heat release rate (T_{PHRR}) of the P(3,4)HB/IFR system were shifted to higher temperatures with increasing loading of IFR (shown in Table IV). As shown in Figure 4(b), the PHRR values of the P(3,4)HB/IFR/ZnB system [P(3,4)HB-5∼ P(3,4)HB-7] decreased further with the substitution of part of IFR by ZnB compared to P(3,4)HB-3. Moreover, THR and HRC

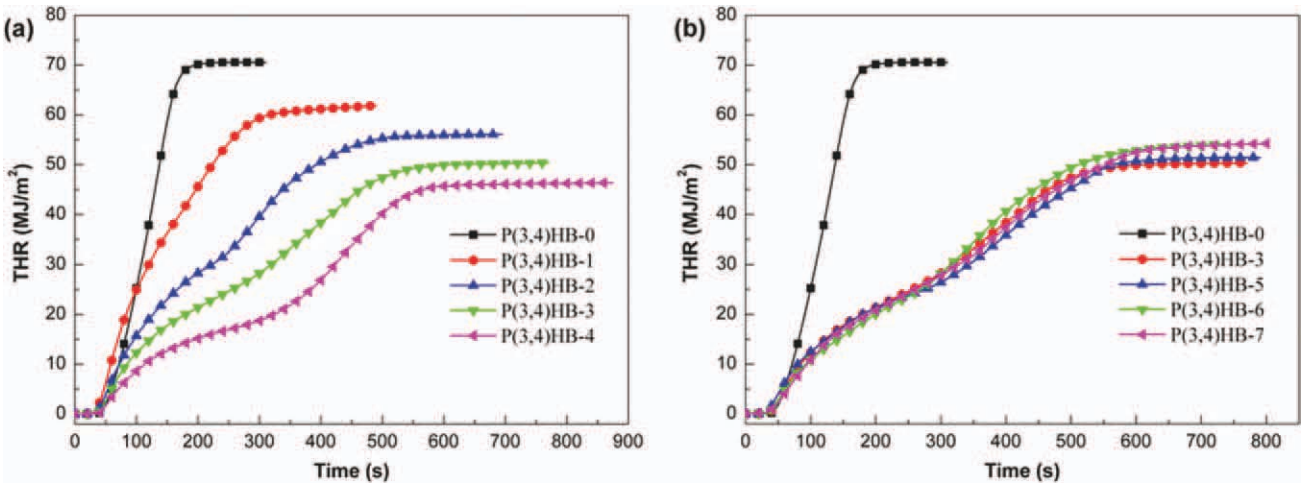

Figure 6 THR curves of the (a) P(3,4)HB/IFR and (b) P(3,4)HB/IFR/ZnB systems obtained from CONE. [Color figure can be viewed in the online issue, which is available at wileyonlinelibrary.com.]

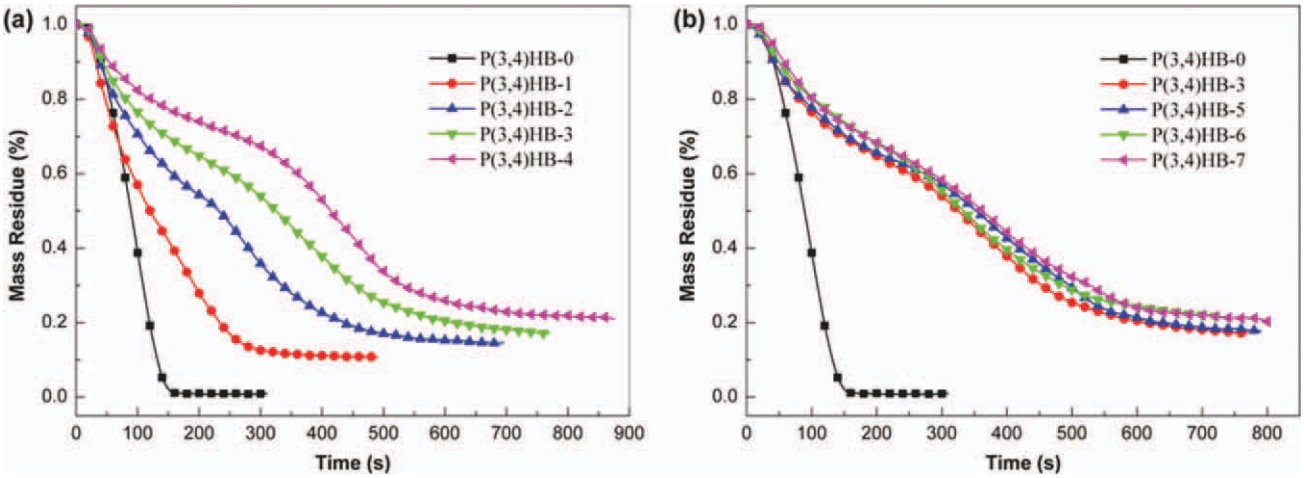

Figure 7 Mass loss curves of the (a) P(3,4)HB/IFR and (b) P(3,4)HB/IFR/ZnB systems obtained from CONE. [Color figure can be viewed in the online issue, which is available at wileyonlinelibrary.com.]

of the P(3,4)HB/IFR/ZnB system were also both reduced in comparison to those of P(3,4)HB-3 because of the synergistic effects of ZnB. All MCC data indicated that IFR cooperating with ZnB effectively reduced the risk of fire of P(3,4)HB.

CONE testing

Data derived from CONE are presented in Figures 5–7, and the combustion parameters obtained from CONE are listed in Table V. The HRR curves for each sample are shown in Figure 5. It can be seen that P(3,4)HB-0 burned fast after ignition, and a sharp PHRR appeared with a PHRR value of 711 kW/m^2 (as shown in Fig. 5). Like the results obtained from MCC, in the presence of P(3,4)HB/IFR with or without ZnB, the PHRR values were greatly reduced. In addition, the HRR curves of the P(3,4)HB/IFR and P(3,4)HB/IFR/ZnB systems evolved from one to two peaks. The first peak could be attributed to the development of intumescent protective char, and the second peak could be ascribed to the degradation of the protective char.[27]

It can be seen from Table V that the time to ignition (TTI) of the flame retardant P(3,4)HB was shorter than that of neat P(3,4)HB; this was due to the development of the intumescent protective char. The burning times of these blends were all prolonged in comparison with that of P(3,4)HB-0. The THR and mass loss curves are presented in Figures 6 and 7, respectively. As shown in Figure 6(a), THR decreased continuously from 71 MJ/m^2 for P(3,4)HB-0 to 46 MJ/m^2 for P(3,4)HB-4. However, the THR values of the P(3,4)HB/IFR/ZnB system were slightly higher than those of P(3,4)HB-3, and the combustion time was also longer; this indicated that the char formed could not bear the high temperature for longer times, as compared to P(3,4)HB-3. Although the P(3,4)HB/IFR/ZnB system had no significant effect on THR compared to P(3,4)HB-3, its THR values were still far lower than that of P(3,4)HB-0. These lower THR values suggested that a part of the P(3,4)HB/IFR, with or without ZnB, had not burned completely. At the end of combustion, there was little residual char left (1%) for neat P(3,4)HB, and the residual char increased with the addition of IFR [shown in Fig. 7(a)]. Finally, P(3,4)HB-4 with 30 wt % IFR had 21% residual char. When part of the IFR in P(3,4)HB-3 was substituted by ZnB, the residual char of P(3,4)HB/IFR/ZnB increased further to 18, 21, and 21% for P(3,4)HB-5, P(3,4)HB-5, and P(3,4)HB-7, respectively, in comparison with that of P(3,4)HB-3 [shown in Fig. 7(b)]. The lower mass loss indicated that the char formed was more efficient for suppressing the transfer of mass and heat.

Char residue analysis

The morphologies of the char residue from the samples after LOI testing were analyzed further by SEM, as shown in Figure 8. As shown in Figure 8(a,b), the

TABLE V
Combustion Parameters Obtained from CONE

Sample	PHRR (kW/m^2)	Av-HRR (kW/m^2)	TTI (s)	THR (MJ/m^2)	Mass (%)
P(3,4)HB-0	711	247	22	71	1
P(3,4)HB-1	466	130	14	62	11
P(3,4)HB-2	299	83	17	56	15
P(3,4)HB-3	245	67	20	50	17
P(3,4)HB-4	180	54	22	46	21
P(3,4)HB-5	242	67	16	51	18
P(3,4)HB-6	198	76	19	54	21
P(3,4)HB-7	193	69	20	54	21

Av-HRR, Average heat release rate.

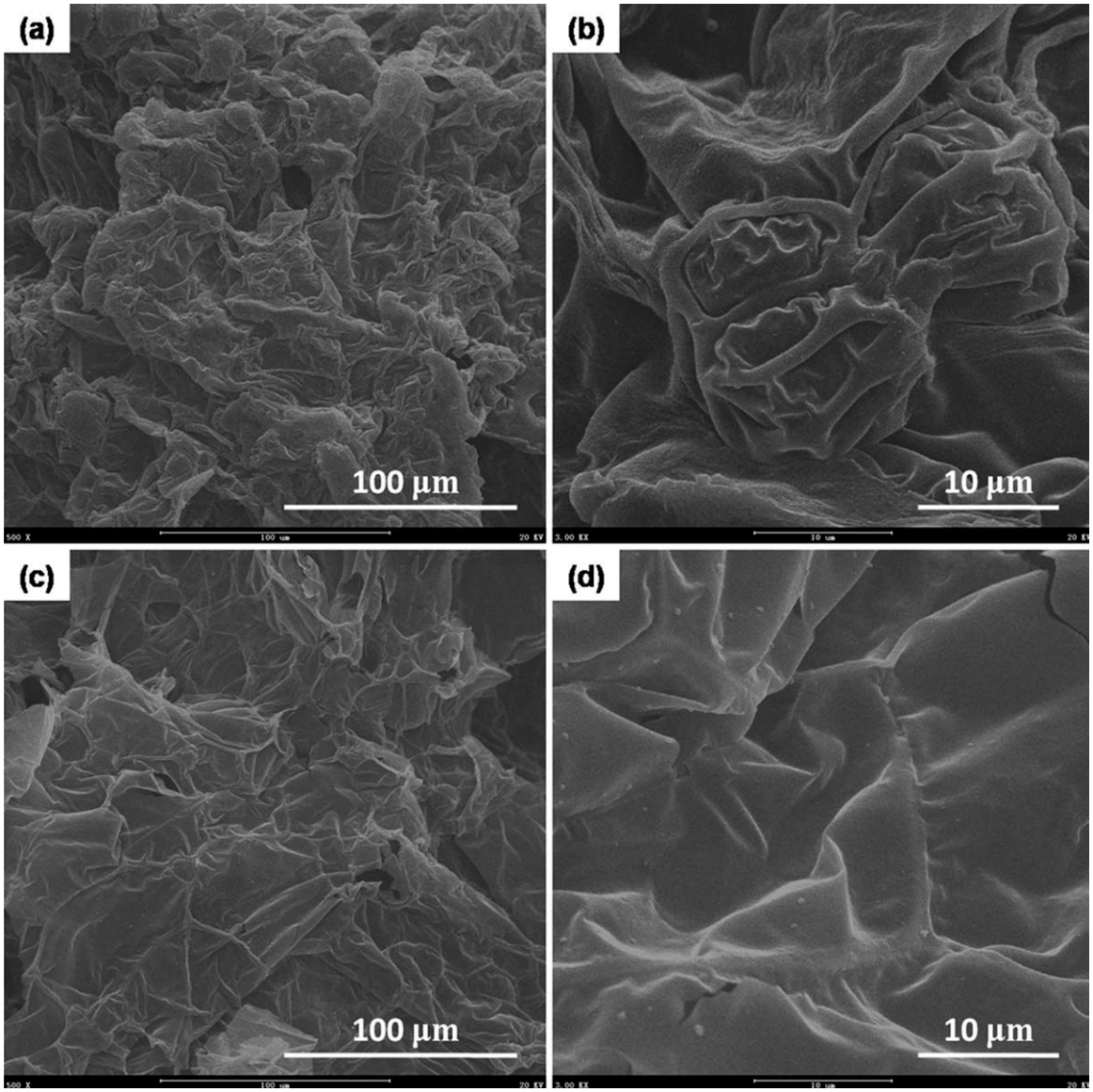

Figure 8 SEM images of residues from the (a,b) P(3,4)HB-3 and (c,d) P(3,4)HB-5 composites.

char residue of P(3,4)HB-3 had a good char structure as a barrier to heat and mass transfer during combustion. However, there were quite a few wrinkles on the surface of the char residue, and they were apt to crack. With the addition of ZnB to the P(3,4)HB/IFR system, the morphology of the char residue was obviously changed. Compared with P(3,4)HB-3, a continuous, dense, and more solid intumescent charring layer was formed for P(3,4)HB-5 [Fig. 8(c,d)]. This was because ZnB was a kind of low-melting-point glass body and had a sealing effect on the pores and cracks of the fresh char. Upon combustion, ZnB can generate B_2O_3 to form glassy film on the surface of a matrix.[22,23] So the quality of the char residue of P(3,4)HB/IFR/ZnB was superior to that of P(3,4)HB/IFR. The better quality of char residue played a key role in the synergist flame-retardant effect of ZnB on P(3,4)HB/IFR.

CONCLUSIONS

In this work, IFR combined with ZnB was used to develop a biobased P(3,4)HB material with improved flame retardancy. The results from combustion testing show that the LOI value of the P(3,4)HB/IFR with 0.5 wt % of ZnB increased to 28 $\pm$ 0.5, and this was higher than that of P(3,4)HB/IFR, whose LOI was 27 $\pm$ 0.5. Meanwhile, the UL 94 rating of P(3,4)HB/IFR was improved with the addition of 0.5–2 wt % ZnB (from V-1 to V-0). The TGA results indicate that the char yields and the thermal stability of the char at high temperature of the P(3,4)HB/IFR samples, with or without ZnB, were higher than that of neat P(3,4)HB, and the maximum decomposition rate temperature of these samples was also higher compared with that of neat P(3,4)HB. The data of TG–FTIR showed that the

main products of the thermal decomposition of P(3,4)HB were CO_2, unsaturated ester, unsaturated carboxyl acid, and propene. The flammable gas products released during the thermal degradation process were greatly decreased. The results of MCC and CONE showed that the PHRR, HRC, and mass loss were significantly reduced with the addition of IFR, and these values of the P(3,4)HB/IFR system decreased further when a small amount of IFR was substituted by ZnB. The SEM images demonstrated that more compact char residues were present because of the incorporation of ZnB.

References

1. Yu, L.; Dean, K.; Li, L. Prog Polym Sci 2006, 31, 576.
2. Khanna, S.; Srivastava, A. K. Process Biochem 2005, 40, 607.
3. Bucci, D. Z.; Tavares, L. B. B.; Sell, I. Polym Test 2005, 24, 564.
4. Dagnon, K. L.; Chen, H. H.; Innocentini-Mei, L. H.; D'souza, N. A. Polym Int 2009, 58, 133.
5. Williams, S. F.; Martin, D. P.; Horowitz, D. M.; Peoples, O. P. Int J Biol Macromol 1999, 25, 111.
6. Sainter, P.; Tajalli, K.; Ipsita, R. J Chem Technol Biotechnol 2007, 82, 233.
7. Li, S. M.; Ren, J.; Yuan, H.; Yu, T.; Yuan, W. Z. Polym Int 2010, 59, 242.
8. Levchik, S. V.; Weil, E. D. Polym Int 2005, 54, 11.
9. Gao, F.; Tong, L. F.; Fang, Z. P. Polym Degrad Stab 2006, 91, 1295.
10. Li, S. M.; Yuan, H.; Yu, T.; Yuan, W. Z.; Ren, J. Polym Adv Technol 2009, 20, 1114.
11. Horacek, H.; Pieh, S. Polym Int 2000, 49, 1106.
12. Duquesne, S.; Magnet, S.; Jama, C.; Delobel, R. Surf Coat Technol 2004, 180–181, 302.
13. Yi, D. Q.; Yang, R. J. J Appl Polym Sci 2010, 118, 834.
14. Réti, C.; Casetta, M.; Duquesne, S.; Bourbigot, S.; Delobel, R. Polym Adv Technol 2008, 19, 628.
15. Li, J.; Wei, P.; Li, L. K.; Qian, Y.; Wang, C.; Huang, N. H. Fire Mater 2011, 35, 83.
16. Giúdice, C. A.; Benítez, J. C. Prog Org Coat 2001, 42, 82.
17. Wu, N.; Yang, R. J. Polym Adv Technol 2009, 22, 495.
18. Wu, Z. P.; Shu, W. Y.; Hu, Y. C. J Appl Polym Sci 2007, 103, 3667.
19. Wu, Z. P.; Hu, Y. C.; Shu, W. Y. J Appl Polym Sci 2010, 117, 443.
20. Wu, Z. P.; Hu, Y. C.; Shu, W. Y. J Vinyl Addit Technol 2009, 15, 260.
21. Fontaine, G.; Bourbigot, S.; Duquesne, S. Polym Degrad Stab 2008, 93, 68.
22. Dogan, M.; Yılmaz, A.; Bayramlı, E. Polym Degrad Stab 2010, 95, 2584.
23. Samyn, F.; Bourbigot, S.; Duquesne, S.; Delobel, R. Thermochim Acta 2007, 456, 134.
24. Gu, J. W.; Zhang, G. C.; Dong, S. L.; Zhang, Q. Y.; Kong, J. Surf Coat Technol 2007, 201, 7835.
25. Li, S. D.; He, J. D.; Yu, P. H.; Cheung, M. K. J Appl Polym Sci 2003, 89, 1530.
26. Wang, X.; Hu, Y.; Song, L.; Xuan, S. Y.; Xing, W. Y.; Bai, Z. M.; Lu, H. D. Ind Eng Chem Res 2011, 50, 713.
27. Bourbigot, S.; Bras, M. L.; Delobel, R.; Bréant, P.; Tremillon, J. M. Polym Degrad Stab 1996, 54, 275.